High-Resolution Solid-State NMR Investigation of the Phase Transition in Decamethylferrocene−Acenaphthenequinone Charge-Transfer Complex

Hideaki Nakamura,[†,‡] Daisuke Kuwahara,[*,‡] and Tomoyuki Mochida[§]

The University of Electro-Communications, 1-5-1 Chofugaoka, Chofu-shi, Tokyo 182-8585, Japan, and Department of Chemistry, Graduate School of Science, Kobe University, Rokkodai, Nada, Kobe 657-8501, Japan

Received: June 12, 2009; Revised Manuscript Received: October 10, 2009

A charge-transfer complex composed of decamethylferrocene (D) and acenaphthenequinone (A) was prepared. The material was a 1:1 neutral complex with a mixed-stack structure and exhibited a phase transition at −16 °C. High-resolution ^{13}C and ^{1}H NMR spectroscopy revealed that an inclination of A with respect to D occurs below the phase-transition temperature. The ^{1}H spin-diffusion rates of the complex undergoing high-speed magic-angle spinning (MAS) were measured to determine the shortest $^{1}H-^{1}H$ distance r between D and A. To analyze the experimental results, we derived the analytical expression of the spin-diffusion rate W_z for a homonuclear multispin system undergoing MAS. It was found that W_z for the complex is proportional only to $1/r^6$ under high-speed MAS conditions. On the basis of this relationship and the crystal structure at 20 °C, it was determined that the shortest $^{1}H-^{1}H$ distance r at −27.7 °C (below the phase transition temperature) is 0.4 Å shorter than that at 20 °C. Given this information, a plausible model of the low-temperature structure is discussed.

1. Introduction

Molecular materials exhibit various dynamical behaviors in the solid state, such as molecular motions, structural changes, and phase transitions.[1] In particular, molecular motions of metallocenes in the solid state have been a topic of interest; metallocenes and metallocenium salts often exhibit dynamically disordered phases.[2−5] Metallocene-based charge-transfer (CT) complexes have attracted special attention from the viewpoint of molecular magnetism.[6,7] To date, we have synthesized many ferrocene-based CT complexes[8−10] and supermolecules.[11−15] Elucidation of the molecular motions in metallocene-based materials is also important in connection with their electronic functions. The dynamics of metallocene derivatives have been investigated by various methods including crystallography, thermal analyses, Mössbauer spectroscopy, and solid-state NMR spectroscopy.

In this study, a charge-transfer complex composed of decamethylferrocene (D) and acenaphthenequinone (A) was prepared. Figure 1 shows the structural formula of this complex. Except for strong acceptors such as DDQ (2,3-dichloro-5,6-dicyano-1,4- benzoquinone),[16−19] quinone derivatives are generally weak acceptors and should give neutral complexes, exhibiting only a slight degree of charge-transfer. The decamethylferrocene−acenaphthenequinone complex is indeed a neutral complex, which results from acenaphthenequinone being a weak acceptor.[20] Although neutral CT complexes are less important than ionic CT complexes from the viewpoint of their electronic properties, they should be suitable for investigating the relationship between structure and molecular motion by means of solid-state NMR. In terms of molecular motions, since acenaphthenequinone has a planar and symmetric structure, its complexes should have low internal degrees of freedom in the solid state.

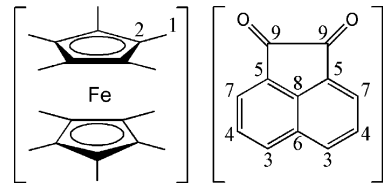

Figure 1. Structural formula of decamethylferrocene−acenaphthenequinone complex. Numbering scheme of the carbon sites is shown.

Differential scanning calorimetry (DSC) experiments on the decamethylferrocene−acenaphthenequinone complex have shown that a phase transition occurs at −16 °C. Although the crystal structure of the complex was determined at 20 °C by X-ray diffraction analysis, structure determination below the phase transition temperature was unsuccessful. This is likely due to disorder or twinning in the crystals on a macroscopic scale. In this study, to elucidate the change in structure or molecular motions associated with the phase transition, we apply high-resolution solid-state NMR methods to this complex. The molecular motions are examined by ^{1}H T_1 measurements. To elucidate the change in structure around the phase transition, we specifically focus on ^{1}H spin-diffusion experiments under high-speed magic-angle spinning (MAS) conditions and the data analysis of these experiments.

In the theory section, we focus on deriving an analytical expression for the spin-diffusion rate of a homonuclear multispin system undergoing MAS. This is performed to obtain information on the $^{1}H-^{1}H$ distances between D and A. In Results and Discussion, we present a new model for a ^{1}H multispin system in the solid state. The analytical expression modified for this model enables us to determine the shortest $^{1}H-^{1}H$ distance between D and A by a simple algebraic calculation. Most

* Corresponding author. Phone: +81-42-443-5730. Fax: +81-42-443-5732. E-mail: kuwahara@cia.uec.ac.jp.
† Present address: Mitsubishi Materials Corporation, 5 Mitacho, Yokkaichi-shi, Mie 510-0841, Japan; E-mail: nhideaki@mmc.co.jp.
‡ The University of Electro-Communications.
§ Kobe University.

10.1021/jp905508r CCC: $40.75
Published on Web 10/26/2009

conventional NMR studies using ^{1}H spin diffusion in the solid state have investigated domain diameters in materials of interest, and the lower limit is about 5 Å.[21] On the other hand, using the analytical expression based on the new model, we can determine changes in the shortest ^{1}H−^{1}H distance, and there is no inherent limit on the scale of the distance information obtained.

In this paper, we use the term "lower temperatures" to refer to temperatures lower than the phase transition temperature and use the term "higher temperatures" to refer to temperatures higher than the phase transition temperature. The intermolecular ^{1}H distances between D and A at lower temperatures are estimated in order to elucidate the structural change that occurs around the phase transition.

2. Experimental Section

Decamethylferrocene and acenaphthenequinone were purchased from Aldrich and used without further purification. The 1:1 charge-transfer complex was obtained as black block crystals by slow evaporation of dichloromethane solutions of a mixture of the two components. Anal. Calcd. for $C_{32}H_{36}O_2Fe$: C, 75.58; H, 7.13. Found: C, 75.50; H, 7.05. NMR spectra were recorded on a Tecmag Apollo spectrometer (operating at 75.431 MHz for ^{13}C and 299.9515 MHz for ^{1}H) equipped with a Doty XC MAS 4 mm probehead. ^{13}C cross-polarization magic angle spinning (CP/MAS) experiments[22,23] were performed with the following parameters: a 4 μs ^{1}H-$\pi/2$ pulse, a 50 kHz CP field strength, a 1 ms CP time, and a 7 s recycle delay. A two-pulse phase-modulation (TPPM) decoupling sequence,[24] with a 65 kHz decoupling field and ±12.5° phase-modulation angles, was used. ^{1}H spin-diffusion experiments[25,26] were performed with a three-pulse sequence [$\pi/2$(a soft pulse)-$\pi/2$(a hard pulse)-τ-$\pi/2$(a hard pulse)-acquisition], using a 4.0 μs hard pulse. To selectively excite one resonance with the first $\pi/2$ pulse, we employed a Gaussian soft pulse[27] of 1.5 ms. The recycle delay of this pulse sequence was 7 s. ^{1}H spin−lattice relaxation times (T_1) were determined using the inversion−recovery technique. ^{1}H high-resolution NMR spectra were measured by using a two-dimensional phase-modulated Lee−Goldburg (2D PMLG) pulse sequence.[28] The variation of the sample spinning speed ν_r was less than ±20 Hz in all MAS experiments. Temperatures of the sample were detected by a thermocouple on the inside near the air inlet of the probe housing, which were corrected with the ^{79}Br spin−lattice relaxation times of KBr powder.[29] Infrared spectra were recorded on a JASCO FT-IR 230 spectrometer as KBr pellets. UV−vis spectra were recorded on a JASCO V-570 UV−vis/NIR spectrometer; diffuse reflectance spectra were measured for polycrystalline samples and Kubelka−Munk conversion was applied to the spectra. Single-crystal X-ray diffraction data were collected on a Bruker SMART APEX CCD diffractometer using Mo Kα radiation (λ = 0.71073 Å) at 293 K. The structure was solved by direct method and refined by using SHELX-97.[30] The non-hydrogen atoms were refined anisotropically. Crystallographic parameters include orthorhombic, space group *Cmcm*, with unit cell a = 15.0066(1) Å, b = 8.6813(8) Å, c = 20.4088(1) Å, and V = 2,658.8(4) Å^3; Z = 4, D_{calcd} = 1.270 g cm^{-3}, $R_1(I > 2\sigma(I))$ = 0.0979, wR_2 = 0.3230, 1764 independent reflections (R(int) = 0.0312), and 100 parameters refined on F^2. DSC measurements were performed using a TA Instruments Q100 differential scanning calorimeter in the temperature range 170−370 K at a scan rate of 10 K min^{-1}.

3. Theory

The ^{1}H magnetization transfer from D to A is observed in this study. High-resolution ^{1}H NMR measurements are necessary to observe this magnetization transfer; these measurements can be performed by using high-speed MAS. Furthermore, we acquire the ^{1}H spin-diffusion rate by analyzing the time-dependence of the ^{1}H magnetization transfer. The spin-diffusion rate W_z for a homonuclear multispin system, as is well-known, depends on the homonuclear dipolar interactions.[21] Hence, once we determine the spin-diffusion rate W_z, we can obtain information on internuclear distances in the spin system. When the equation relating W_z to those internuclear distances is known, there is the possibility of determining the distances. In this section, we will briefly describe the derivation of the analytical expression of the spin-diffusion rate W_z. In addition, a simple and powerful method using the analytical expression to extract the distance information regarding the homonuclear spins will be presented in the next section.

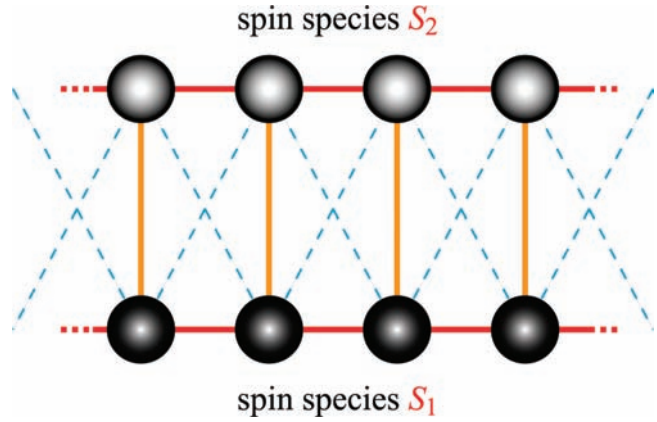

Figure 2. Schematic representation of a homonuclear multispin system in the solid state. This model system was employed by Suter et al. to derive the analytical expression of the spin-diffusion rate between S_1 and S_2 under sample stationary condition.

Let us consider a solid that contains homonuclear spin species, S_1 and S_2, contributing to separate resonance lines (Figure 2). This is a model system for ^{1}H multispin systems and has been studied by Suter et al.[31] It was assumed in their study that this model system has strong dipolar couplings within each species and weaker dipolar couplings between the two species (Figure 2). They derived an analytical expression describing the spin-diffusion rate W_z between S_1 and S_2 under the stationary sample condition. The expression of W_z had the dipolar coupling constant d_c associated with r in an explicit form. In these cases, it is in principle possible to determine the corresponding internuclear distance r through numerical calculation with the double-quantum spectrum for S_1 and S_2 (the measurement of the double-quantum spectrum of S_1 and S_2 is required).

Several publications[31−38] have presented analytical rate expressions for the magnetization transfer that occurs in various spin systems. Among them, the treatment by Suter et al.[31] using the above model system is considered to be suitable for describing the ^{1}H magnetization transfer in the decamethylferrocene−acenaphthenequinone complex, since D and A yield two resolved ^{1}H resonance lines under high-speed MAS conditions. Unfortunately, the analytical expression derived by Suter et al. is applicable to only the stationary state of the sample; therefore, it is required to derive the expression under sample spinning conditions. In this study, we employed the calculation treatment presented by Kubo et al.[35] in order to derive the analytical expression of the spin-diffusion rate W_z for the above model system (Figure 2) undergoing MAS.

Kubo et al.[35] have studied the case of spectral spin-diffusion between two rare spins-1/2 S_A and S_B (e.g., ^{13}C−^{13}C) in the

presence of abundant I spins (e.g., ^{1}H's) in a solid. They derived an analytical expression of the spin-diffusion rate W_z between S_A and S_B under MAS conditions. It is worth noting that the expression of W_z contains not only the dipolar coupling constant d_c (between S_A and S_B) but also the free induction decay (FID) signals corresponding to S_A and S_B. As a result, this analytical expression has the advantage that the spin-diffusion rate W_z can be calculated without measuring the double-quantum NMR spectrum of S_A and S_B.

In the case of spectral spin diffusion in the model system in Figure 2, when the spin system undergoes MAS, the spin-diffusion rate between S_1 and S_2 is given by the following expression:

$$W_z = -\frac{1}{15} d_c^2 \int_0^\infty G(\omega_r, \tau)(f_0(\tau)\cdot g_0^*(\tau) + f_0^*(\tau)\cdot g_0(\tau))d\tau \quad (1)$$

where

$$G(\omega_r, \tau) = \frac{1}{2} \sum_{n=\pm1,\pm2} \exp\{in\omega_r\tau\} \quad (2)$$

and

$$d_c = \gamma_S^2 \hbar / r^3 \quad (3)$$

Here, γ_s is the gyromagnetic ratio of spins S_1 and S_2, $\hbar$ is the Plank constant, r is the internuclear distance between S_1 and S_2, ω_r is the sample spinning speed, and f_0 and g_0 represent the FID signal functions for S_1 and S_2, respectively. We succeeded in deriving the above expression (eq 1) based on the work of Kubo et al.[35] An important point to note is that in deriving eq 1 we have taken into account only one type of interspecies interaction (i.e., the dipolar interactions given by the nearest-neighbor internuclear distance r). The remaining weaker interactions can be treated analogously and give additive contributions to the spin-diffusion rate.

Using the results of eqs 1−3, we can calculate the ^{1}H−^{1}H internuclear distances between D and A, although in practice numerical calculation of eq 1 is somewhat troublesome. However, in the following section, it is shown that, in some cases, the distance information can be easily extracted on the basis of this analytical expression (eq 1).

4. Results and Discussion

The decamethylferrocene−acenaphthenequinone complex was obtained as black crystals by recrystallization from dichloromethane. The UV−vis absorption spectra of the complex exhibited a very broad band between 500 and 1100 nm, which is assignable to the charge-transfer band, while no absorption was observed above 550 nm in either decamethylferrocene or acenaphthenequinone. In the infrared region, the C═O stretching band of the complex was observed at 1720 cm^{-1}, which is the same frequency as that of neutral acenaphthenequinone. This indicates that the complex is neutral and the degree of charge-transfer is only slight, which is consistent with the weak electron affinity of the acceptor. DSC measurements revealed that the complex exhibits a first-order phase transition at 257.2 K, accompanied by a hysteresis of 6.0 K (ΔH = 1.9 kJ mol^{-1} and ΔS = 7.4 J K^{-1} mol^{-1}). No other phase transitions were detected.

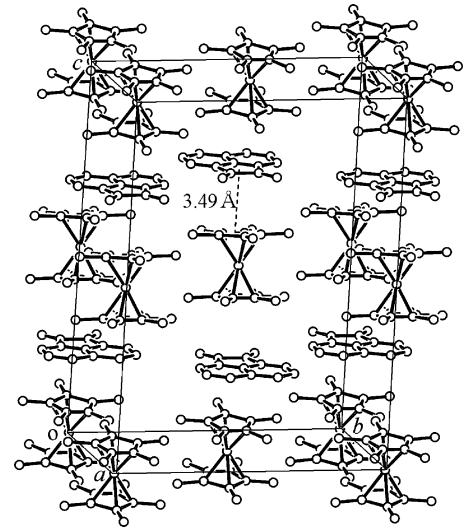

Figure 3. Crystal structure of the complex at 20 °C. Hydrogen atoms are omitted for clarity.

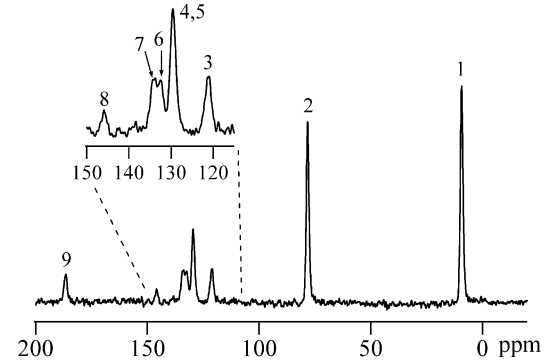

Figure 4. ^{13}C CP/MAS NMR spectrum of the complex at room temperature. This spectrum was measured under a sample spinning speed of 5 kHz.

Figure 3 shows the crystal structure of the complex determined at 20 °C by X-ray diffraction analysis. The D/A stoichiometry is 1:1. Along the c axis, the donors and the acceptors are stacked alternately, forming a mixed-stack structure (Cp−Acenaphthenequinone distance: 3.49 Å). Each molecule is located on an inversion center, and the intramolecular bond lengths are comparable to those observed in neutral compounds.[39,40] Although the overall structure seems to be essentially correct, care should be taken because the R value was high (R = 0.979), and the molecular structure had large thermal ellipsoids. Furthermore, structure determination below the phase transition temperature was unsuccessful, and the crystal system could not be determined. We suspect that these phenomena may be related to molecular motion, disorder, or twinning, which are likely associated with the phase transition. Therefore, to examine whether changes in molecular motion or orientation occur at the phase transition, we performed a microscopic investigation using solid-state NMR.

Figure 4 is the ^{13}C CP/MAS NMR spectrum measured at room temperature using a sample spinning speed of 5 kHz. The line integrations (not shown) of all resonance lines were determined by ^{13}C single pulse and ^{1}H decoupling NMR experiments. The resonance lines corresponding to quaternary carbons were confirmed through a dipolar-dephasing NMR experiment.[41] The assignment of each resonance line, which was made on the basis of these two experimental results, is written alongside each signal in Figure 4.

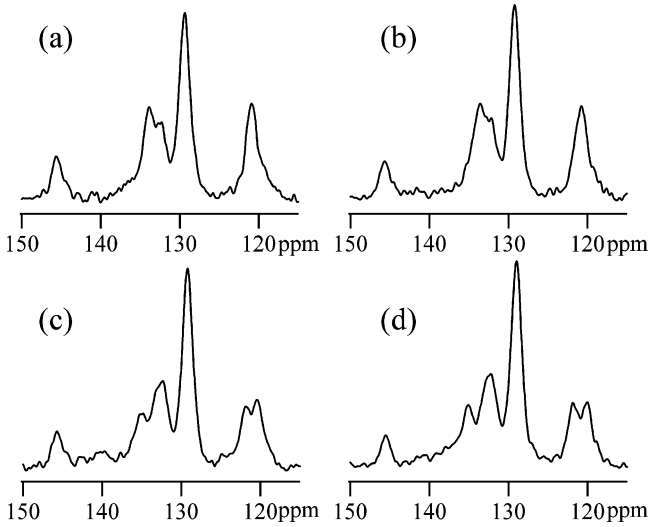

Figure 5. ^{13}C CP/MAS NMR spectra of the complex at (a) 1.3 °C, (b) −18.7 °C, (c) −28.7 °C, and (d) −48.7 °C. The NMR signals in the range of 115−150 ppm which are assigned to ^{13}C nuclei of acenaphthenequinone are displayed.

TABLE 1: ^{13}C Chemical Shift Data for the C3 Carbons of the Complex

temperature (°C)	δ (ppm)
1.3	120.9
−18.7	120.8
−28.7	121.9; 120.4
−48.7	122.0; 120.2

Figure 5 shows the ^{13}C CP/MAS NMR spectra in the range of 115−150 ppm. These spectra were measured at temperatures in the range of −48.7 to 1.3 °C using a sample spinning speed of 5 kHz. At the temperature of −28.7 °C, a splitting of the resonance lines corresponding to C3 was found. For reference, we measured the ^{13}C NMR spectra of acenaphthenequinone in the same temperature range (not shown in this publication) and confirmed that no splittings were observed. We conclude from this result that there is an essential interaction between D and A that yields the splitting patterns in the ^{13}C NMR spectra at lower temperatures.

Table 1 summarizes the chemical-shift values of the C3 carbons at various temperatures. The peak of the C3 carbons at a higher temperature is located almost centrally between the two peaks that are observed at a lower temperature. More precisely, the peak at a higher temperature is located nearer the peak with a low frequency between the two peaks that are observed at a lower temperature. This suggests that the two peaks at lower temperatures merged at higher temperatures because of oscillating motion between two sites. It is likely that the oscillating motion freezes at lower temperatures and A becomes inclined with respect to D.

To confirm this expectation, that is, the inclination of A with respect to D, we performed the 2D PMLG experiments at −36.8 and 3.2 °C to acquire high-resolution ^1H NMR spectra (Figure 6). In Figure 6b, line splitting of the ^1H resonance line for the methyl protons of D is clearly visible, which demonstrates that the ^1H nuclei in the donor above and below the acceptor plane are in different environments. This is consistent with the above picture.

The variation of ^1H spin−lattice relaxation times T_1 with temperature are plotted in Figure 7. These data were acquired at temperatures in the range of −68 to 31 °C using a sample spinning speed of 12 kHz. The circles and squares represent

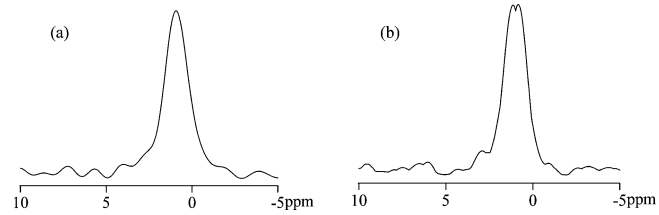

Figure 6. High-resolution ^1H NMR spectra for the complex at (a) 3.2 °C and (b) −36.8 °C. These ^1H NMR spectra were measured using the 2D PMLG pulse sequence. The signal intensities of the protons of A are very small compared to those of the methyl protons of D. The former signals are buried in noise, and only the signals for the methyl protons of D are visible in these spectra.

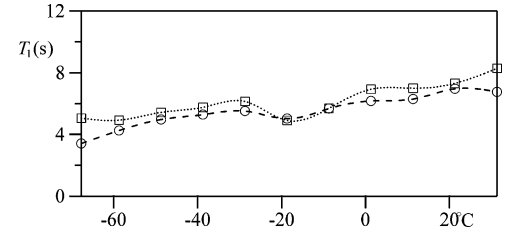

Figure 7. Variation of ^1H spin−lattice relaxation times T_1 with temperature. These data were acquired using a sample spinning speed of 12 kHz. The circles and squares represent the ^1H T_1 times of D and A in the complex, respectively.

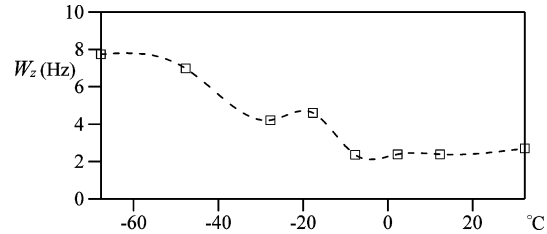

Figure 8. Variation of the ^1H spin-diffusion rates between D and A in the complex with temperature. These data were acquired using a sample spinning speed of 12 kHz.

the ^1H T_1 times of D and A, respectively. The two kinds of ^1H T_1 times exhibit a gradual decrease with decreasing temperature, but the orders of both T_1 times are unchanged in the temperature range. It appears that molecular motions, such as the rotation of methyl groups of D or the rotational jump around the C_5 axis of D,[42] show little change in this temperature range. This is consistent with the small entropy change observed in the DSC measurements, which indicate that there are no order−disorder-like phenomena.

Figure 8 shows the variation of the ^1H spin-diffusion rates of the complex with temperature. It shows an almost flat line from room temperature to the vicinity of the phase transition temperature. Near the phase transition temperature, the ^1H spin-diffusion rate exhibits an appreciable increase. After passing the phase transition temperature, it shows a gradual increase with decreasing temperature. In subsequent paragraphs, we estimate intermolecular distances and molecular orientations in the low temperature phase by analyzing these results.

In the model system of the ^1H multispin system in Figure 2, there are many vertical lines connecting the subsystems S_1 and S_2. These vertical lines are made up of dipolar interactions, and their lengths are given by a constant r; that is, the model system in Figure 2 is characterized by one nearest-neighbor internuclear distance r between S_1 and S_2. On the other hand, the decamethylferrocene−acenaphthenequinone complex has several nearest-neighbor $^1H-^1H$ (S_1-S_2) distances between D and A. Figure 9 depicts this situation. In this study, we employed

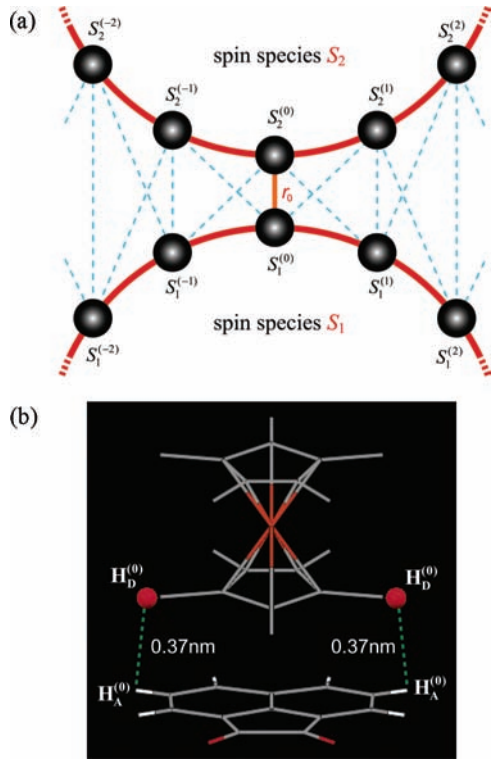

Figure 9. (a) Model system used to determine the ^{1}H internuclear distances between D and A in this study. Lines connecting nuclear spins show dipolar interactions; different kinds of lines depict the assumptions made in this study (see text). (b) Shortest ^{1}H−^{1}H distance r_0 between D and A at 20 °C.

somewhat rough assumptions to estimate the structures at lower temperatures. They are as follows (see Figure 9a): (i) The dipolar interaction between $S_1^{(0)}$ and $S_2^{(0)}$, which has the shortest nearest-neighbor distance r_0, provides the dominant contribution to the spin-diffusion rate W_z, such that the remaining contributions from other types of dipolar interactions can be omitted. (ii) Each of the subsystems reaches thermal equilibrium at a rate of $1/\tau_{eq}$, much shorter than the spin-diffusion rate W_z, such that the nuclear spin $S_1^{(0)}$ and the other spins in the subsystem S_1 have a common polarization at each step of the diffusion periods τ (the diffusion periods τ used to determine the spin-diffusion rates were τ = 10 m, 50 m, 100 m, ...). The same assumptions apply to $S_2^{(0)}$ and the subsystem S_2. (iii) It was assumed that the three methyl protons of each methyl group were situated at the intersection of the plane of ^{1}H rotation and the rotation axis (methyl protons undergo rapid rotation, in general).

Under these assumptions, the spin-diffusion rate W_z is described by eq 1 with the exception that d_c is given by $d_c^{(0)} = \gamma_S^2\hbar/r_0^3$, where r_0 is the internuclear distance between $S_1^{(0)}$ and $S_2^{(0)}$. In the decamethylferrocene−acenaphthenequinone complex, r_0 is 3.7 Å at 20 °C. This is the distance between the proton nucleus bonded to the C7 carbon and a proton nucleus in D (see Figure 9b). We denote the former proton as $H_A^{(0)}$ and the latter proton as $H_D^{(0)}$. It should be noted that $H_A^{(0)}$ and $H_D^{(0)}$ correspond to $S_1^{(0)}$ and $S_2^{(0)}$ in Figure 9a.

Using the model system in Figure 9a and the above assumptions, we can now estimate the internuclear distance $H_A^{(0)} - H_D^{(0)}$ by numerically calculating W_z; however, this troublesome work is not necessary in this study. The analytical expression eq 1 has two independent terms: the first term depends on the dipolar coupling constant between $S_1^{(0)}$ and $S_2^{(0)}$, and the second term depends on the sample spinning speed ν_r ($=\omega_r/2\pi$) as well as the two FID signals of $S_1^{(0)}$ and $S_2^{(0)}$ (i.e., D and A). In this study, all the ^{1}H spin-diffusion experiments were carried out at ν_r = 12 kHz. In the temperature range where these experiments were performed (i.e., −68 to 31 °C), little change was observed in the two FID signals of D and A. This means that the second term is unchanged within this temperature range. Hence, the ratio of the spin-diffusion rate at lower temperatures to that at 20 °C is, in this temperature range, given by

$$W_z^{(\text{lower})}/W_z^{(20°\text{C})} = (r_0^{(20°\text{C})})^6/(r_0^{(\text{lower})})^6 \quad (4)$$

where $W_z^{(\text{lower})}$ and $W_z^{(20\ °\text{C})}$ are the spin-diffusion rates at lower temperatures and at 20 °C, respectively. Therefore, we can obtain the ^{1}H internuclear distance through a simple calculation with eq 4. It is important that the dependence of W_z on the internuclear distances is the same as that observed in the nuclear Overhauser effect;[43] that is, the $1/r^6$ dependence of magnetization transfer rates holds in the case of ^{1}H spin-diffusion in the decamethylferrocene−acenaphthenequinone complex undergoing high-speed MAS.

Equation 4 indicates that, when the ^{1}H internuclear distance at a given temperature is known, we can easily estimate the internuclear distances at other temperatures from the analytical calculations based on eq 4. For example, the internuclear distance between $H_A^{(0)}$ and $H_D^{(0)}$ determined according to eq 4 is 3.3 Å at −27.7 °C. The internuclear distances decrease by 0.4 Å around the phase transition temperature. This decrease is interpreted as resulting from the inclination of the A plane with respect to D, as discussed above. Shrinkage of the crystal lattice constants can be neglected; we confirmed that the length of the c axis at 90 K (20.382 Å) was only slightly shorter than that at 293 K (20.409 Å).

It has been reported that pure decamethylferrocene performs five-site jumps around the C_5 axis at temperatures of −160 °C or higher.[42] In order to investigate the molecular motion of D in the complex, we measured static ^{13}C NMR spectra of the complex in the temperature range from −60 to 20 °C. The ^{13}C NMR spectra of the C2 carbons exhibited an axially symmetric powder pattern, which indicates that the D molecules in the complex are also performing five-site jumps at least in this temperature range. However, even when the D molecules in the complex are undergoing five-site jumps, methyl protons can be considered to always be located at the $H_D^{(0)}$ position (see Figure 9b). Therefore, the proposed analytical approach (which is based on the model system in Figure 9a and eqs 1−4) is applicable to the analysis of the spin-diffusion rates of this complex, thus enabling determination of the $H_A^{(0)}$−$H_D^{(0)}$ distances of this complex at lower temperatures.

We will now examine inclinations of the A plane from a mechanical standpoint. For simplicity, we consider the inclinations about the axes passing through the center of gravity (CG), which is located in close proximity to the C8 site (Figure 10). The coordinates are (0 Å, 0.3 Å). The inclination of the A plane (or a rotation of the A plane) is defined by the following two terms: the line around which the A plane is tilted and the angle of tilt. The inclinations around lines in the vicinity of the y axis may occur when the moments of inertia of the molecule are considered. However, inclination around only the y axis or the x axis can be excluded from consideration because such inclination does not yield the splitting of the resonance lines at the C3 sites.

Figure 11a shows the local molecular arrangement viewed along the b axis in the crystal structure of the complex at 20 °C (Figure 11a is a part of the crystal structure at 20 °C). On the

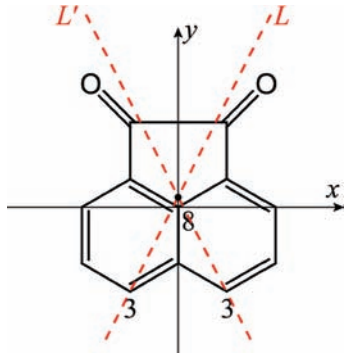

Figure 10. Structural formula of A showing the rotation axis. The dot just above the C8 site is the center of gravity of the molecule.

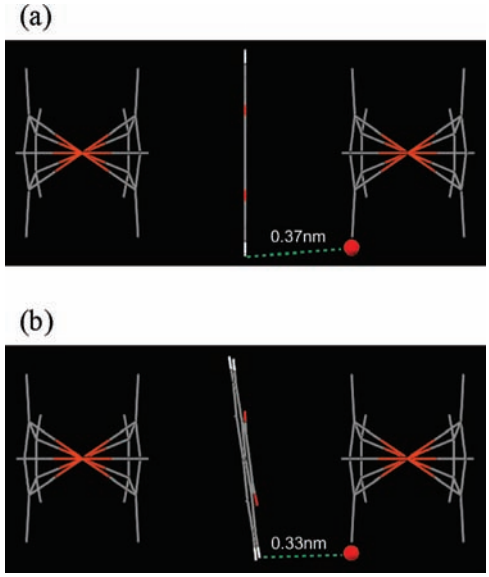

Figure 11. (a) Molecular arrangement in the complex, based on the X-ray data at 20 °C. (b) Plausible molecular arrangement at −27.7 °C. This configuration was produced by tilting the acenaphthenequinone plane around line *L* in Figure 10 such that the $H_A^{(0)}-H_D^{(0)}$ distance is 3.3 Å.

other hand, Figure 11b shows an example of the crystal structures that were generated only by the A plane inclinations in Figure 11a. Figure 11b was determined in such a way that the $H_A^{(0)}-H_D^{(0)}$ distance was 3.3 Å under the rotation of the A plane around line *L* in Figure 10. (Note that rotation around line *L′* yields the same result.)

For Figure 11b, the rotation angle of the A plane around line *L* is 8.7°. On the other hand, the rotation of the A plane around *L* by −8.7° in Figure 11a yields the same potential energy as the configuration in Figure 11b. Therefore, it seems reasonable that at higher temperatures there is an oscillating motion between these two sites. This can fundamentally explain the chemical-shift values of the C3 carbons observed at various temperatures (see Table 1). However, the oscillation around line *L* makes the position of one of the C3 carbons invariant (see Figure 10). Thus, it is thought that the real rotation axis deviates slightly from line *L* (or *L′*) shown in Figure 10 toward the *y* axis. In this case, when the oscillation freezes at a lower temperature, one of the two peaks of the C3 carbons at that temperature should have a chemical shift closer to that of one peak at a higher temperature. In fact, the peak of the C3 carbons at a higher temperature is situated nearer the peak with a low frequency between the two peaks that are observed at a lower temperature. This supports the above hypothesis, namely, deviation of the real rotation axis.

In conclusion, the configuration shown in Figure 11b is plausible at lower temperatures, although this model may be overly simplified. Indeed, the inclination of A may accompany the inclination of D, and the real structure would be more complicated. Furthermore, the NMR observations relate only to the local structure, while long-range disorder, mismatch, or incommensurate structures probably occur on the macroscopic scale. The model presented here is a simple model that satisfies the NMR observations.

5. Conclusion

We prepared a neutral CT complex composed of decamethylferrocene and acenaphthenequinone and investigated the local structure of the complex by using high-resolution solid-state NMR methods. The proposed structure is based on an analysis of the ^{1}H spin-diffusion rates and observations of the ^{13}C and ^{1}H NMR spectra. The phase transition of the complex was related to the change of the molecular motion of A and the resultant change of the molecular arrangement, which is consistent with the entropy change observed in the DSC measurements. First-order phase transitions are often observed in metallocenium salts, and this study may provide insights into structural changes in such materials.

In this study, to obtain information on the ^{1}H−^{1}H distances between D and A, we specifically focused on deriving an analytical expression for the spin-diffusion rate of a homonuclear multispin system undergoing MAS. This is because the analytical expressions presented to date for such a spin system are those for the stationary sample conditions. Hence, in this study, it was necessary to derive the analytical expression of the spin-diffusion rate of such a spin system under MAS conditions.

The analytical expression derived here consists of a dipolar coupling constant and an integral term. The integrand consists of FID signal functions of two resolved resonance lines among which the polarization transfer takes place. Therefore, in principle the spin-diffusion rate can be calculated without any special information such as double-quantum NMR spectra, which are necessary for the general calculations to determine spin-diffusion rates. In addition, we presented a new model for a ^{1}H multispin system in the solid state. Using the analytical expression modified for this model, we could determine the shortest ^{1}H−^{1}H distance between D and A by a simple algebraic calculation. Applications of the analytical expression (presented in this study) based on this new model will therefore be of great utility for elucidating changes in the structure of various molecular materials in the solid state.

Supporting Information Available: Derivation of eq 1, DSC data, ^{1}H MAS NMR spectrum measured at room temperature at a sample spinning speed of 12kHz, fitting curves for the ^{1}H spin-diffusion rates at various temperatures, discussion about the numbers of the methyl and the aromatic protons of the complex, and static ^{13}C NMR spectra of the complex at several temperatures. This material is available free of charge via the Internet at http://pubs.acs.org.

References and Notes

(1) *Structure Correlation*; Burgi, H.-B., Dunitz, J. D., Eds.; VCH: London, 1996.
(2) Schottenberger, H.; Wurst, K.; Greisser, U. J.; Jetti, R. K. R.; Laus, G.; Herber, R. H.; Nowik, I. *J. Am. Chem. Soc.* **2005**, *127*, 6795–6801.
(3) Braga, D.; Grepioni, F. *Chem. Soc. Rev.* **2000**, *29*, 229–238.
(4) Webb, R. J.; Lowery, M. D.; Shiomi, Y.; Sorai, M.; Wittebort, R. J.; Hendrickson, D. N. *Inorg. Chem.* **1992**, *31*, 5211–5219.
(5) Bérar, J. -F.; Calvarin, B.; Weigel, D. *J. Chem. Phys.* **1980**, *73*, 438–441.

(6) Miller, J. S.; Epstein, A. J.; Reiff, W. M. *Angew. Chem., Int. Ed. Engl.* **1994**, *33*, 385–415, and references therein.

(7) *Ferrocenes: Homogenous Catalysis, Organic Synthesis, Materials Science*; Togni, A., Hayashi, T., Eds.; Wiley-VCH: Weinheim, Germany, 1995, Chapter 8, and references therein.

(8) Mochida, T.; Koinuma, T.; Akasaka, T.; Sato, M.; Nishio, Y.; Kajita, K.; Mori, H. *Chem.—Eur. J.* **2007**, *13*, 1872–1881.

(9) Mochida, T.; Takazawa, K.; Takahashi, M.; Takeda, M.; Nishio, Y.; Sato, M.; Kajita, K.; Mori, H.; Matsushita, M. M.; Sugawara, T. *J. Phys. Soc. Jpn.* **2005**, *74*, 2214–2216.

(10) Mochida, T.; Yamazaki, S.; Suzuki, S.; Shimizu, S.; Mori, H. *Bull. Chem. Soc. Jpn.* **2003**, *76*, 2321–2328.

(11) Mochida, T.; Shimuzu, F.; Shimizu, H.; Okazawa, K.; Sato, F.; Kuwahara, D. *J. Organomet. Chem.* **2007**, *692*, 1834–1844.

(12) Horikoshi, R.; Nambu, C.; Mochida, T. *New J. Chem.* **2004**, *28*, 26–33.

(13) Horikoshi, R.; Ueda, M.; Mochida, T. *New. J. Chem.* **2003**, *27*, 933–937.

(14) Horikoshi, R.; Mochida, T.; Moriyama, H. *Inorg. Chem.* **2002**, *41*, 3017–3024.

(15) Mochida, T.; Okazawa, K.; Horikoshi, R. *Dalton. Trans.* **2006**, 693–704.

(16) Yee, G. T.; Whitton, M. J.; Sommer, R. D.; Frommen, C. M.; Reiff, W. M. *Inorg. Chem.* **2000**, *39*, 1874–1877.

(17) Miller, J. S.; Glatzhofer, D. T.; O'Hare, D. M.; Reiff, W. M.; Chakraborty, A.; Epstein, A. J. *Inorg. Chem.* **1989**, *28*, 2930–2939.

(18) Salman, H. M. A.; Mahmoud, M. R.; Abou-El-Wafa, M. H. M.; Rabie, U. M.; Crabtree, R. H. *Inorg. Chem. Commun.* **2004**, *7*, 1209–1212.

(19) Yee, G. T.; Whitton, M. J.; Sommer, R. D.; Frommen, C. M.; Reiff, W. M. *Inorg. Chem.* **2000**, *39*, 1874–1877.

(20) Ge, Y.; Miller, L.; Ouimet, T.; Smith, D. K. *J. Org. Chem.* **2000**, *65*, 8831–8838.

(21) Schmidt-Rohr, K.; Spiess, H. W. *Multidimensional solid-state NMR and polymers*; Academic Press: London, 1994.

(22) Pines, A.; Gibby, M. G.; Waugh, J. S. *J. Chem. Phys.* **1972**, *56*, 1776–1777.

(23) Schaefer, J.; Chin, S. H.; Weissman, S. I. *Macromolecules* **1972**, *5*, 798–801.

(24) Bennett, A. E.; Rienstra, C. M.; Auger, M.; Lakshmi, K. V.; Griffin, R. G. *J. Chem. Phys.* **1995**, *103*, 6951–6958.

(25) McBrierty, V. J. *Polymer* **1974**, *15*, 503–520.

(26) McBrierty, V. J.; Douglass, D. C. *J. Polymer Sci., Macromol. Rev.* **1981**, *16*, 295–366.

(27) Bauer, C.; Freeman, R.; Frenkiel, T.; Keeler, J.; Shaka, A. J. *J. Magn. Reson.* **1984**, *58*, 442–457.

(28) Vinogradov, E.; Madhu, P. K.; Vega, S. *Chem. Phys. Lett.* **1999**, *314*, 443–450.

(29) Thurber, K. R.; Tycko, R. *J. Magn. Reson.* **2009**, *196*, 84–87.

(30) Sheldrick, G. M. *Acta Crystallogr.* **2008**, *A64*, 112–122.

(31) Suter, D.; Ernst, R. R. *Phys. Rev. B* **1985**, *32*, 5608–5627.

(32) McArthur, D. A.; Hahn, E. L. *Phys. Rev.* **1969**, *188*, 609–638.

(33) Henrichs, P. M.; Linder, M.; Hewitt, J. M. *J. Chem. Phys.* **1986**, *85*, 7077–7086.

(34) Kubo, A.; McDowell, C. A. *J. Chem. Phys.* **1988**, *89*, 63–70.

(35) Kubo, A.; McDowell, C. A. *J. Chem. Soc., Faraday Trans. 1* **1988**, *84*, 3713–3730.

(36) Eckman, R.; Pines, A.; Tycko, R.; Weitekamp, D. P. *Chem. Phys. Lett.* **1983**, *99*, 35–40.

(37) Robyr, P.; Meier, B. H.; Ernst, R. R. *Chem. Phys. Lett.* **1989**, *162*, 417–423.

(38) Briuand, J.; Ernst, R. R. *Chem. Phys. Lett.* **1991**, *185*, 276–285.

(39) Freyberg, D. P.; Robbins, J. L.; Raymond, K. N.; Smart, J. C. *J. Am. Chem. Soc.* **1979**, *101*, 892–897.

(40) Mak, T. C. W.; Trotter, J. *Acta Crystallogr.* **1963**, *16*, 811–815.

(41) Opella, S. J.; Frey, M. H. *J. Am. Chem. Soc.* **1979**, *101*, 5854–5856.

(42) Wemmer, D. E.; Ruben, D. J.; Pines, A. *J. Am. Chem. Soc.* **1981**, *103*, 28–33.

(43) Wagner, G.; Wüthrich, K. *J. Magn. Reson.* **1979**, *33*, 675–680.

JP905508R